Traditional vs Generative Design Optimization for Novel Wrist Exoskeleton

Federico Mariano[1,2,*], Roberto Francesco Pitzalis[1,2], Luigi Monica[3], Jesus Ortiz[2] and Giovanni Berselli[1,2]

[1]*DIME, Università di Genova*, Genoa, Italy
[2]*ADVR, Istituto Italiano di Tecnologia*, Genoa, Italy
[3] *Department of Technological Innovation and Safety Equipment, INAIL*, Rome, Italy

federico.mariano@iit.it, roberto.pitzalis@iit.it, l.monica@inail.it,
jesus.ortiz@iit.it, giovanni.berselli@unige.it

***Abstract*—This paper will focus on two possible optimizations for a novel wrist exoskeleton. Exoskeletons are structures designed to support human joints using mechanical components and are used in various fields such as rehabilitation, military, and industrial sectors. The study focuses on a new exoskeleton for the wrist with the intention of optimizing its weight and mechanical strength. Two optimization methods are employed. the first one aims to achieve traditional optimization using Computer-Aided Design (CAD) and Finite Element Method (FEM) analysis. In the second the use of Generative Design (GD) optimization, which combine topological optimization and Artificial Intelligence (AI), wants to create new organic components almost impossible to obtain without using this tool. The results indicate that GD optimization significantly reduces maximum displacement while maintaining stress levels within material limits, often improving the weight of the part. Moreover, GD optimization streamlines the design process, offering quicker iterations than traditional methods. This study highlights the efficacy of GD in achieving superior exoskeleton designs with improved mechanical properties and reduced weight, presenting it as a valuable tool for designers seeking optimal solutions in less time.**

***Index Terms*—Generative Design, Exoskeleton, FEM analysis**

I. Introduction

The term exoskeleton has two different meanings, depending on the field of application. In nature, it corresponds to the outer covering that protects many animals, such as insects and shellfishes [1]. In robotics, it is a structure that covers and supports the joints of a human using mechanical joints and, sometimes, motors to facilitate movements [2]. In this paper, we refer to robotics when we talk about exoskeletons. These devices were used for many different purposes, such as rehabilitation [3]–[7], military [8], and industrial [9], [10]. Rehabilitation exoskeletons must assist patients with limited movements due to neurological or musculoskeletal disorders, such as stroke, incidents, and bone fractures [3]–[5]. Military exoskeletons want to improve the physical ability of the soldier, preventing injuries without blocking any required movements in the field [8]. Finally, the industrial exoskeleton should follow the worker's movements during their tasks to prevent any injuries or problems that might affect them in daily working activities [9], [10].

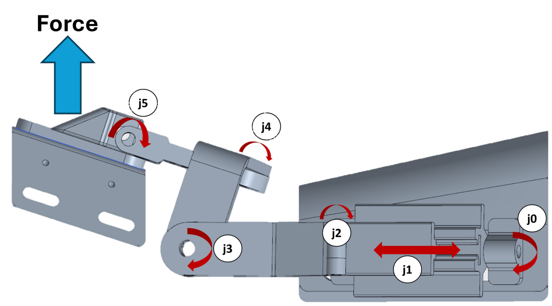

Fig. 1. Lateral view of the wrist exoskeleton highlighting joints and applied simulated force

Today, it is possible to distinguish among three different exoskeleton types: Active, passive, and quasi-passive. Links and joints in **passive** devices are connected by components that store potential energy, such as springs. This stored energy is then utilized to facilitate the necessary movements. This exoskeleton type is widely used in rehabilitation as it does not require complex systems such as motors and sensors. In fact it is generally lightweight and allows usage in hospitals and independently at home [3] [11] [12]. On the other hand, **active** exoskeletons use external sources to move joints and links [6] [13] [5]. The sources are generally motors or levers, which can be positioned close to the joints or take advantage of cables and belts by being able to position the actuators away from the links. In fact, by placing the motors away from the joints, there is an improvement in weight distribution, increasing the ergonomics of the device [14], [15]. Finally, an exoskeleton that integrates both of these features is considered a **quasi-passive** system [16] [17].

This study focuses on a novel wrist exoskeleton (As shown in Fig. 1) and its optimization to find the best compromises in weight and mechanical strength. This device was made using 3D printing and ABS as material, and it was optimized using a force of 10 N directed vertically over the palm. Since

* For further contact *federicomariano.mariano@polimi.it*, DEIB, Politecnico di Milano.

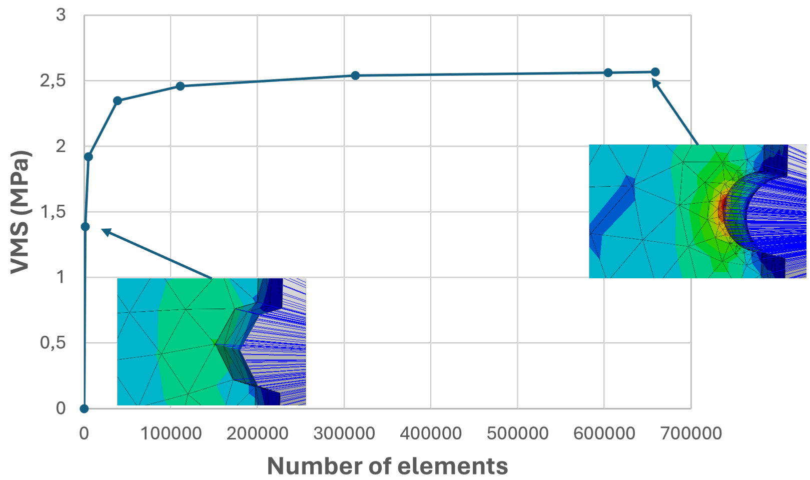

Fig. 2. Graph showing the trend of the tensional state of an object as the number of elements increases.

the interface between the user and the exoskeleton is constructed from rigid materials, it classifies as a rigid exoskeleton [14]. Indeed, these devices can also be differentiated by the stiffness of their components. Materials with high stiffness, such as steel, alluminium, or hard plastics like ABS, form rigid systems [14]. If, on the other hand, softer materials, such as rubbers, silicones, and soft plastic, are used, we talk about soft exoskeletons [13] [18]. Rigid exoskeletons have the advantage of ensuring high efficiency on transmission, while soft exoskeletons are able to adapt better to the skin, ensuring better contact and ergonomics [14].

The paper is divided in the following way.

Section 2 discusses how to produce an appropriate FEM analysis and optimization methods, which is carried out in two different ways. The first follows a traditional approach, while the second uses Generative Design (GD) optimization. In Section 3, the optimization results will be analyzed, and the main stress, displacements, and weight involving different parts will be compared. Section 4 will discuss the results, and finally, Section 5 will present the conclusion about how to make proper optimization and comparisons between different strategies, highlighting the pros and cons.

II. Materials and Methods

A. FEM analyses

The finite element method (FEM) is an advanced numerical technique used in engineering and mathematical problems applied to static or dynamic components [19]. This procedure approximates solutions of differential and integral equations that describe physical phenomena such as stress analysis, heat transfer, fluid dynamics, and electromagnetism. The method divides a complex problem into more minor, straightforward elements or subregions that are easier to analyse. FEM starts by dividing the problem domain into smaller, interconnected subdomains called finite elements. These elements can be of different shapes, such as triangles, quadrilaterals, tetrahedrons, or hexahedrons, with various accuracy. The dimension of the mesh is crucial to find the best solution possible. The smaller the object's size, the closer the solution reaches the actual value, following an asymptotic trend (As shown in Fig. 2) [20].

A set of nodes, called also point cloud, defines each finite element.

The entire system's behavior is approximated by assembling the behavior of these smaller elements using calculus and linear algebra. The software transforms the continuous problem into a discrete problem. This involves representing the unknown function by a series of values at discrete points within each element. The discrete equations for each element are then assembled into a global system of equations, taking into account boundary conditions and constraints of the overall problem. Once the system of equations is formed, it can be solved using numerical techniques like matrix inversion, iterative solvers, or direct solution methods. FEM analysis finds application in diverse scenarios, including structural analysis [21], multibody dynamics [22], heat transfer [23], acoustics [24], and vibrations [25]. This study specifically aims to determine the VMS and maximum displacement using Recurdyn, a multibody dynamics software.

This software offers a variety of element types for simulation purposes [26].

- **Solid4 (linear function)**: This type of element is made up of 4 nodes that form linear tetrahedrons (Fig. 3.a). Tetrahedrons are preferred in FEM analysis due to their ability to model complex geometries efficiently [27]. Each node in a Solid4 element has 3 degrees of freedom, corresponding to translations along the X, Y, and Z axes in the Cartesian coordinate system.
- **Solid8 (linear function)**: The Solid8 element is a brick-shaped entity known as a linear hexahedron, which is made up of eight interconnected nodes (Fig. 3.b). Like Solid4, each node has 3 translational degrees of freedom

in the coordinate system.
- **Solid10 (quadratic function)**: The Solid10 element is an extension of the Solid4 type, featuring 10 nodes instead of 4 (Fig. 3.c). These nodes include 4 corner nodes and 6 edge nodes, offering a more refined mesh.

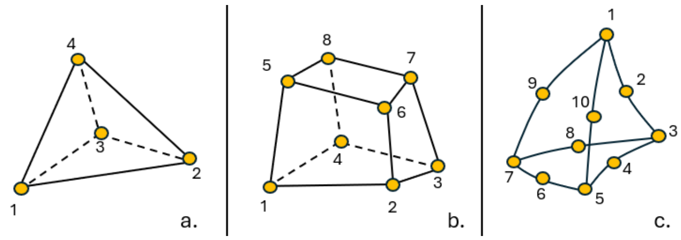

Fig. 3. Different type of meshes used in Recurdyn. a) Solid4. b) Solid8. c) Solid10.

In Recurdyn, linear function meshes calculate the effective stress field at the nodes, with stress values interpolated linearly between nodes. While this method accurately calculates deformations and displacements at this points, the interpolated values between them are approximations, potentially diverging from reality as the distance between nodes increases. Reducing the mesh size can improve accuracy but increases computation time. A strategic approach is to reduce the mesh size only in critical high-stress areas.
Alternatively, quadratic elements, like Solid10, can provide more realistic simulations using second-degree functions, though they require more nodes and longer simulation times. For this study the simulation was made using Solid4 as a type of mesh trying to locally decrease the minimum size of each element so as not to explode the calculation time needed to derive the stress of Von Mises and the minimum displacement. In addition, all simulations were also checked to be sure that they had arrived at convergence.

B. No optimised prototype

The exoskeleton described in this chapter has been designed for industrial application, to assist workers during their daily tasks.
The device was designed with active components to assist and enhance wrist flexion-extension movements. This type of movement allows 150° hand rotation divided into 80° during flexion and 70° in extension [28]. The flexion of the hand allows the approach of the palm to the arm, while during the extension of it has a removal of the palm resulting in the approach of the back (As shown in Fig. 4). Its design has been preliminary evaluated and defined through the use of virtual prototyping software Creo Parametric. This papers describes the device from the point of view of mechanical and structural design without going into details about what is the actuation system and its characteristics.
Nine parts form the main structure of the system, connected using one active and five passive joints (As shown in Fig. 1, and Tab. I). ABS was chosen as material choice because the organic design required by GD optimization needs the use of 3d printing as fabrication method. It is also true that there are 3D printers that use other materials, such as titanium or stainless steel, but few institutes or universities have the possibility to use this machinery.

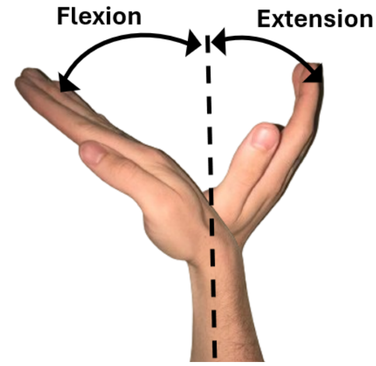

Fig. 4. Flexion-extension movement.

TABLE I
JOINTS USED IN THE EXOSKELETON

Joints	Type	Description
J0, J2, J3, J5	Passive revolute	Allows the movements desired by the worker
J1	Passive prismatic	Allows elongation of the skin
J4	Actuated revolute	Connected to the motors and helps the flex-extension

For the optimization, we chose to modify the Linkage Inversion Lever (connecting from J2 to J3), the Inversion Lever (connecting from J3 to J4), and then the Hinge support (connecting from J4 to J5).
The first step consists of a FEM analysis of the three parts in order to find VMS and the maximum displacement under external forces.
As preliminary evaluation, a force of 10N has been set, which is low for a proper optimization. This choice was due to the material used. ABS is a plastic material and has poor mechanical properties compared with other materials such as steel or alluminium [29] [30]. Nevertheless, the Eq. 1, 2 and 3 shows that the force has a linear contribution concerning stress and displacements. If results are to be obtained for higher force values, it is only needed to calculate displacement and stress by making a simple comparison.
The force was set vertically over the palm (As shown in Fig. 1), and the results were obtained using Recurdyn, a Multi-Body Dynamics software.

C. Traditional optimization

In order to achieve the best performance possible, we have undertaken the task of modifying several key parameters of the individual parts. This involved adjusting the fillets, holes, and thickness of each component to strike a balance between reducing weight and maintaining desirable mechanical properties.

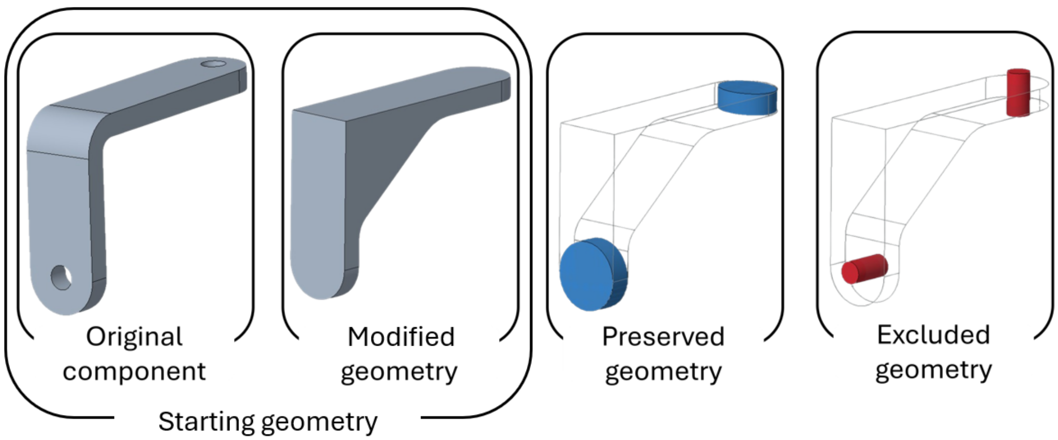

Fig. 5. Geometries used to realize GD optimization on Inversion Lever

The modifications were determined using the Creo Parametric CAD software, which allowed us to precisely alter the design and evaluate the effects of these changes. Following this, the Recurdyn Multibody software was used to perform a further detailed analysis. This included calculating the VMS and measuring the maximum displacement, ensuring that our design modifications met the necessary performance criteria.

D. Generative Design optimization

Generative design works using simultaneously topological optimization and AI.

The first paper concerning topological optimization was written in 1988 by Bendsøe and Kikuchi [31]. The primary question behind the creation of this optimization was "What is the optimal shape of structural elements?". The GD uses AI tools to show the designer many solutions to this question.

GD made iterative optimization, reducing an objective function, which could be the part's mass, until it finds the best solution. This approach can lead to creating objects that are not only strong in terms of mechanical properties but also difficult to imagine and almost impossible to obtain without using this particular tool [32].

For this study, Creo Parametric software were used to create the parts and then verify the VMS and the maximum displacements obtained using this solution.

The steps to optimize the components are straightforward [33]. First, the designer may use three geometries (As shown in Fig. 5).

- **Starting geometry:** Generally, this is the original geometry of the part. If the designer wants to get a more robust object, it is recommended to modify the unoptimized geometry to increase the workspace. The GD will then modify these volumes to obtain the best shape possible.
- **Preserved geometry:** The user must use the surfaces of the preserved geometry to set loads and constraints. Creo Parametric will not modify this volume. It is mandatory that this geometry must be fully contained in the starting geometry to perform the optimization.
- **Excluded geometry:** These volumes are unnecessary to create the GD optimized part. However, if part of the component needs to be removed, the software can delete these occupied volumes from the original component.

Using Creo Parametric software, the designer can apply forces, moments, pressures, centrifugal forces and linear accelerations as loads.

Instead, available constraints include:

- Fixed: Prevents a selected surface from moving or deforming.
- Displacement: Creates an obligatory translational displacement in a specified direction for a selected surface.
- Planar: Allows full planar motion of flat surfaces.
- Cylindrical: A cylindrical constraint controls the axial movement of a cylindrical surface, allowing angular movement while keeping radial movement fixed.
- Ball: Represents a spherical joint with fixed translation and free rotation.

For this study, the components used were locked using fixed joints, simulating a upward force of 10N, and the moment was calculated starting from the palm.

Another step required to optimize efficiency is setting the design criteria. Within the criteria section, it is possible to maximize the stiffness of the part by specifying the percentage of volume to be retained or minimize the mass by including a safety factor. For the analysis, the decision was made to maximize stiffness by limiting the volume used to 60% of the initial geometry's volume.

After completing the above steps, the GD initiates and autonomously executes the optimization by replacing the starting geometry with a new reconstituted geometry formed with a mesh. The speed with which the operation will be completed will be inversely proportional to the number of iterations to complete the optimization. With a larger number of iterations, there is a smaller mesh size with a drastic reduction in sharp edges, but the computation time will increase significantly. The user can choose a level of fidelity ranging from one to ten, where one is a low level of fidelity with increased mesh size, while at ten there will be a decrease regarding the mesh size and thus a move closer to what would be in reality. A level four of fidelity with 256 iterations was used for this optimization. For more information regarding GD optimization, please read the paper by M.Pollák and J. Török [34].

III. Results

Using Recurdyn and Creo Parametric software, results are presented below regarding mass, VMS, and maximum displacement of the Inversion Lever, Linkage Inversion Lever, and Hinge Support. These results are divided into not-modified (Fig. 6.A, fig. 7.A, fig. 8.A), traditionally (Fig. 6.B, fig. 7.B, fig. 8.B) optimised, and GD-optimised (Fig. 6.C, fig. 7.C, fig. 8.C)

Fig. 6. a) Original Inversion Lever, b) Inversion Lever optimized traditionally, c) Inversion Lever GD optimized.

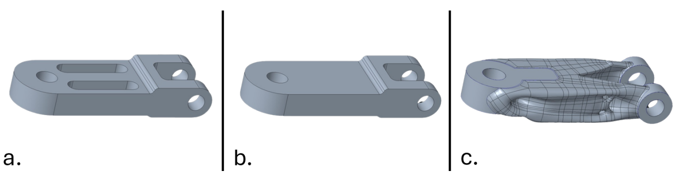

Fig. 7. a) Original Hinge Support, b) Hinge Support optimized traditionally, c) Hinge Support GD optimized.

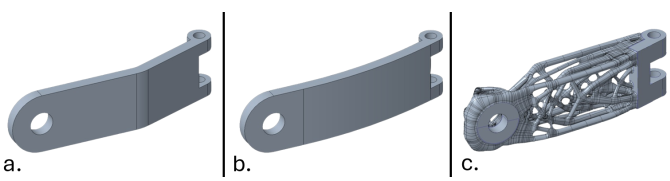

Fig. 8. a) Original Linkage Inversion Lever, b) Linkage Inversion Lever optimized traditionally, c) Linkage Inversion Lever GD optimized.

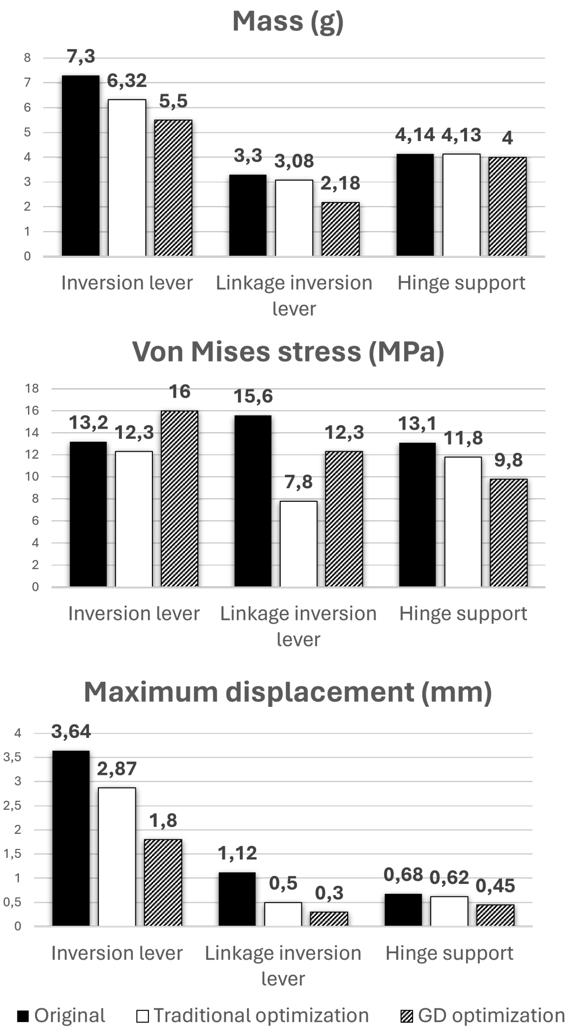

Fig. 9. Histograms regarding results obtained for Inversion Lever, Linkage Inversion Lever and Hinge Support.

A. Inversion Lever

The original inversion lever has a starting mass of 7.3 g, a VMS of 13.2 MPa, and a maximum displacement of 3.64 mm. After the traditional optimization, the mass lowered to 6.32 g, with a value of VMS of 12.3 MPa, and the displacement decreased to 2.87 mm. Using GD optimization, a mass of 5.5 g, a VMS of 16.0 MPa, and a maximum displacement of less then 1.8 mm were obtained.

B. Linkage Inversion Lever

The starting mass of the linkage inversion lever was 3.3 g, with a VMS of 15.6 MPa and a maximum displacement of 1.12 mm. With traditional optimization, the mass of this part results in 3.08 g, a VMS of 7.8 MPa and the maximum displacement was under 0.5 mm. Finally, using the GD tool, it has been found that the mass of the linkage inversion lever was 2.18 g, the VMS was 12.3 MPa, and the displacement was under 0.3 mm.

C. Hinge Support

The last part analyzed in this paragraph is the hinge support. The starting mass, with no modification, was 4.14 g, with a VMS of 13.1 MPa and a maximum displacement of 0.68 mm. After modifications due to the traditional optimization, the mass varies until it reaches 4.13 g, the VMS stabilizes at 11.8 MPa, and the displacement remains at a maximum value of 0.62 mm. Lastly, the GD optimization it was made, finding a mass of 4.0 g, a VMS of 9.8 MPa, and a maximum displacement of 0.45 mm.

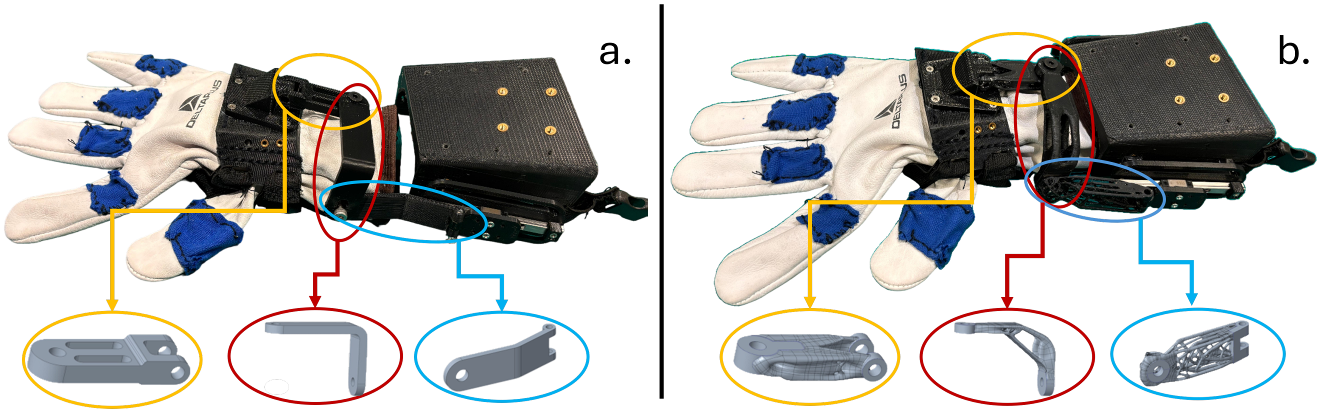

Fig. 10. (a) Exoskeleton without modifications. (b) Exoskeleton after the GD optimization.

IV. Discussion

The first result to analyze is the time spent on the optimization. Using GD, the only trouble was setting the initial conditions, but Creo software made the other steps autonomously. In contrast, traditional optimization requires an iterative step of modifications using CAD software and FEM analyses, which takes more time to perform.

After analyzing the graph of Fig. 10 using traditional optimization, it is possible to notice that there have been improvements regarding the VMS and maximum displacement. On the other hand, mass decreased only for the inversion lever, there was a slightly improvements for linkage inversion lever, while in the case of the hinge support the improvement was practically zero.

Using GD optimization, the best decrease can be seen with respect to the maximum displacement. The VMS decreases for all parts except the Linkage Inversion Lever, which remains under the maximum tolerable stress of ABS [30]. The mass remains almost the same for the Linkage Inversion Lever, and there was a decrease in mass for the other parts.

V. Conclusions

This study compares two optimization strategies made on a wrist exoskeleton.

The first uses traditional optimization to modify the parts and verify the VMS and displacement.

The second one uses GD tools to modify the parts using AI and topology optimization to find the best solution quickly.

Optimizations were performed with a force of 10 N directed vertically over the palm. This choice is due to the material used, ABS, which has poor mechanical characteristics compared to other possible materials. Usually, the creation of objects by taking advantage of GD optimization is carried out using 3D printers. Knowing this, it was decided to use ABS, which appears to be the most commonly used material for this production technique. In addition to this factor, one must also consider the time frame for performing a proper FEM analysis. The time required depends on several factors, such as the size and type of mesh used, the size of the component, and finally, the external force. The greater the simulated force, the greater the computation time. Following this reasoning and because the equations used by Recurdyn software are all linearly dependent on the force, it was decided to limit the value to only 10 N. We needed additional forces with varying angles and modules for better optimization, but we could only use one force for this comparison.

After analyzing the results, the GD optimization performs better and could be considered an essential tool for a designer who wants to create parts that are difficult for a human to obtain.

This solution can improve the design of objects regarding maximum displacement, keeping the VMS below the material limit and sometimes improving the weight of parts. These improvements are achievable by taking less time than traditional optimization.

Acknowledgment

This paper is a shortened version of the author's thesis for Università di Genova [35]. First our thanks go to the XoLab group of Istituto Italiano di Tecnologia (IIT) for their hospitality during the development of this work. Then, we also would like to thank INAIL (Italian Workers Compensation Authority) for its ongoing support, collaboration, and funding in the development of novel types of industrial exoskeletons, under the Collaborative Exoskeletons–EC-2 project in collaboration with IIT and the University of Genoa. Finally, partial funding has been received within the PNC Fit4MedRob - Fit for Medical Robotics project.

References

[1] S. O. Andersen, "Exoskeleton," in *Encyclopedia of insects*. Elsevier, 2009, pp. 339–342.

[2] M. Cenciarini and A. M. Dollar, "Biomechanical considerations in the design of lower limb exoskeletons," in *2011 IEEE International conference on rehabilitation robotics*. IEEE, 2011, pp. 1–6.

[3] S. Ates, C. J. Haarman, and A. H. Stienen, "Script passive orthosis: design of interactive hand and wrist exoskeleton for rehabilitation at home after stroke," *Autonomous Robots*, vol. 41, pp. 711–723, 2017.

[4] C. Lambelet, M. Lyu, D. Woolley, R. Gassert, and N. Wenderoth, "The ewrist—a wearable wrist exoskeleton with semg-based force control for stroke rehabilitation," in *2017 international conference on rehabilitation robotics (ICORR)*. IEEE, 2017, pp. 726–733.

[5] T. Higuma, K. Kiguchi, and J. Arata, "Low-profile two-degree-of-freedom wrist exoskeleton device using multiple spring blades," *IEEE Robotics and Automation Letters*, vol. 3, no. 1, pp. 305–311, 2017.

[6] D. Serrano, D.-S. Copaci, L. Moreno, and D. Blanco, "Sma based wrist exoskeleton for rehabilitation therapy," in *2018 IEEE/RSJ International Conference on Intelligent Robots and Systems (IROS)*. IEEE, 2018, pp. 2318–2323.

[7] G. Vazzoler, P. Bilancia, G. Berselli, M. Fontana, and A. Frisoli, "Preliminary analysis and design of a passive upper limb exoskeleton," 2021, p. 569 – 574.

[8] J. K. Proud, D. T. Lai, K. L. Mudie, G. L. Carstairs, D. C. Billing, A. Garofolini, and R. K. Begg, "Exoskeleton application to military manual handling tasks," *Human Factors*, vol. 64, no. 3, pp. 527–554, 2022.

[9] S. Toxiri, M. B. Näf, M. Lazzaroni, J. Fernández, M. Sposito, T. Poliero, L. Monica, S. Anastasi, D. G. Caldwell, and J. Ortiz, "Back-support exoskeletons for occupational use: an overview of technological advances and trends," *IISE Transactions on Occupational Ergonomics and Human Factors*, vol. 7, no. 3-4, pp. 237–249, 2019.

[10] V. Patel, A. Chesmore, C. M. Legner, and S. Pandey, "Trends in workplace wearable technologies and connected-worker solutions for next-generation occupational safety, health, and productivity," *Advanced Intelligent Systems*, vol. 4, no. 1, p. 2100099, 2022.

[11] S. Sangha, A. M. Elnady, and C. Menon, "A compact robotic orthosis for wrist assistance," in *2016 6th IEEE International Conference on Biomedical Robotics and Biomechatronics (BioRob)*. IEEE, 2016, pp. 1080–1085.

[12] Ottobock, "Paexowrist exoskeleton," https://paexo.com/paexo-wrist/?lang=it, accessed: June 2024.

[13] S. Liu, Z. Fang, J. Liu, K. Tang, J. Luo, J. Yi, X. Hu, and Z. Wang, "A compact soft robotic wrist brace with origami actuators," *Frontiers in Robotics and AI*, vol. 8, p. 614623, 2021.

[14] R. F. Pitzalis, D. Park, D. G. Caldwell, G. Berselli, and J. Ortiz, "State of the art in wearable wrist exoskeletons part i: Background needs and design requirements," *Machines*, vol. 11, no. 4, p. 458, 2023.

[15] ——, "State of the art in wearable wrist exoskeletons part ii: A review of commercial and research devices," *Machines*, vol. 12, no. 1, 2024.

[16] A. M. Dollar and H. Herr, "Design of a quasi-passive knee exoskeleton to assist running," in *2008 IEEE/RSJ international conference on intelligent robots and systems*. IEEE, 2008, pp. 747–754.

[17] K. Shamaei, M. Cenciarini, A. A. Adams, K. N. Gregorczyk, J. M. Schiffman, and A. M. Dollar, "Design and evaluation of a quasi-passive knee exoskeleton for investigation of motor adaptation in lower extremity joints," *IEEE Transactions on Biomedical Engineering*, vol. 61, no. 6, pp. 1809–1821, 2014.

[18] T. Ridremont, I. Singh, B. Bruzek, A. Jamieson, Y. Gu, R. Merzouki, and M. B. Wijesundara, "Pneumatically actuated soft robotic hand and wrist exoskeleton for motion assistance in rehabilitation," in *Actuators*, vol. 13, no. 5. MDPI, 2024, p. 180.

[19] K.-J. Bathe, "Finite element method," *Wiley encyclopedia of computer science and engineering*, pp. 1–12, 2007.

[20] R. Surapureddy, A. Schönning, S. Stagon, and A. Kassab, "Predicting pressure distribution between transfemoral prosthetic socket and residual limb using finite element analysis," *International Journal of Experimental and Computational Biomechanics*, vol. 4, no. 1, pp. 32–48, 2016.

[21] O. C. Zienkiewicz and R. L. Taylor, *The finite element method for solid and structural mechanics*. Elsevier, 2005.

[22] J. Gerstmayr and J. Schöberl, "A 3d finite element method for flexible multibody systems," *Multibody System Dynamics*, vol. 15, pp. 305–320, 2006.

[23] M. V. Reddy, B. Hemasunder, S. Ramana, P. R. Babu, P. Thejasree, and J. Joseph, "State of art on fem approach in inverse heat transfer problems for different materials," *Materials Today: Proceedings*, 2023.

[24] R. Barbieri and N. Barbieri, "Finite element acoustic simulation based shape optimization of a muffler," *applied acoustics*, vol. 67, no. 4, pp. 346–357, 2006.

[25] S.-J. Feng, X.-L. Zhang, Q.-T. Zheng, and L. Wang, "Simulation and mitigation analysis of ground vibrations induced by high-speed train with three dimensional fem," *Soil Dynamics and Earthquake Engineering*, vol. 94, pp. 204–214, 2017.

[26] FunctionBay, Inc., "Help - recurdyn," https://functionbay.com/documentation/onlinehelp/default.htm#!Documents/help.htm, accessed: May 2024.

[27] T. Nguyen-Thoi, G. Liu, K. Lam, and G. Zhang, "A face-based smoothed finite element method (fs-fem) for 3d linear and geometrically nonlinear solid mechanics problems using 4-node tetrahedral elements," *International journal for numerical methods in Engineering*, vol. 78, no. 3, pp. 324–353, 2009.

[28] Y. Youm and A. E. Flatt, "Design of a total wrist prosthesis." *Annals of biomedical engineering*, vol. 12, no. 3, pp. 247–262, 1984.

[29] B. Liu, R. Villavicencio, and C. G. Soares, "Failure characteristics of strength-equivalent aluminium and steel plates in impact conditions," *Analysis and Design of Marine Structures, vol., no*, p. 167, 2013.

[30] H. Jami, S. Masood, and W. Song, "Dynamic stress-strain compressive behaviour of fdm made abs and pc parts under high strain rates," in *IOP Conference Series: Materials Science and Engineering*, vol. 377, no. 1. IOP Publishing, 2018, p. 012153.

[31] M. P. Bendsøe and N. Kikuchi, "Generating optimal topologies in structural design using a homogenization method," *Computer methods in applied mechanics and engineering*, vol. 71, no. 2, pp. 197–224, 1988.

[32] F. Buonamici, M. Carfagni, R. Furferi, Y. Volpe, L. Governi *et al.*, "Generative design: an explorative study," *Computer-Aided Design and Applications*, vol. 18, no. 1, pp. 144–155, 2020.

[33] PTC Inc., "Creo parametric 10.0.4.0 help center," https://support.ptc.com/help/creo/creo_pma/r10.0/italian/#page/introduction/about_PTC_creo_help.html, accessed: May 2024.

[34] M. Pollák and J. Török, "Use of generative design tools in the production of design products using 3d printing technology," *TEM Journal*, vol. 11, no. 1, p. 249, 2022.

[35] F. Mariano, "Virtual prototyping and optimization of an innovative wrist exoskeleton," Genoa, Italy, 2023.